

# Elastic $\alpha$ -transfer in the elastic scattering of $^{16}\text{O}+^{12}\text{C}$

S. Szilner<sup>1,2</sup>, W. von Oertzen<sup>3</sup>, Z. Basrak<sup>1</sup>, F. Haas<sup>2</sup>, and M. Milin<sup>1,3</sup>

<sup>1</sup> Rudjer Bošković Institute, HR-10 002 Zagreb, Croatia

<sup>2</sup> Institut de Recherches Subatomiques, CNRS-IN2P3/ULP, Strasbourg, France

<sup>3</sup> Hahn-Meitner-Institut, 14109 Berlin, Germany

November 23, 2018

**Abstract.** The elastic scattering  $^{16}\text{O}+^{12}\text{C}$  angular distributions at  $^{16}\text{O}$  bombarding energies of 100.0, 115.9 and 124.0 MeV and their optical model description including the  $\alpha$ -particle exchange contribution calculated in the Coupled Reaction Channel approach are presented. The angular distributions show not only the usual diffraction pattern but also, at larger angles, intermediate structure of refractive origin on which finer oscillations are superimposed. The large angle features can be consistently described including explicitly the elastic  $\alpha$ -transfer process and using a refractive optical potential with a deep real part and a weakly absorptive imaginary part.

**PACS.** 25.70.Bc – 25.70.-z – 24.10.Ht

Heavy-ion collisions are generally dominated by strong absorption due to a large number of open channels. This is not the case for certain 'light' heavy-ion systems [1], especially those involving the  $\alpha$ -like nuclei  $^{12}\text{C}$  and  $^{16}\text{O}$ , for which weaker absorption phenomena like molecular resonances [2] and nuclear rainbows [3] have been observed. The observation of the rainbow pattern, the maxima in the differential cross section at the rainbow angle and the associated Airy minima, are closely related to the degree of transparency of the interaction. In systems like  $^{16}\text{O}+^{16}\text{O}$  and  $^{16}\text{O}+^{12}\text{C}$  the regularly spaced sharp minima and broad maxima which move forward in angle as the energy increases have been observed in the angular distributions and have been explained through refractive effects [4, 5, 6, 7, 8]. For systems with non-identical nuclei a significant rise of the elastic cross sections at angles larger than  $90^\circ$  is often accompanied by oscillatory structure [7, 8], which is attributed to elastic transfer [9, 10], a process in which target and projectile exchange their identity by the transfer of their mass difference. In fact, weak absorption or angular momentum dependent absorption can produce effects similar to those due to the exchange scattering. Recently, several studies of cases with refractive scattering in non-identical systems, where the angles beyond  $90^\circ$  can be directly explored, have been published [7, 8, 11, 12].

The elastic angular distributions and the optical model description of the  $^{16}\text{O}+^{12}\text{C}$  system measured at the Strasbourg Vivitron accelerator were reported in Refs. [7, 12, 13]. The main features of the measured angular distributions are the fine forward Fraunhofer diffractive oscillations and the broad structures of refractive origin at larger angles (see also Fig. 1). Of particular interest are the oscil-

lations with a smaller period superimposed on these broad refractive structures at large angles. The main aim of the present study is to investigate the origin of these oscillations and the enhancement of the differential elastic scattering cross section at large angles.

The potentials obtained within the optical model description have deep real parts and weakly absorptive imaginary parts. In our optical model analysis of the Strasbourg data it was shown that an acceptable description was possible using the sum of a volume and a surface term for the imaginary potential. A potential, with only a volume term, describes the main refractive features of the measured distributions but fails to describe the backward-angle cross sections and the oscillations. In the present work the obtained optical potentials, with only a volume term (Table II in Ref. [12]) are used as a phenomenological potential in a Coupled Reaction Channel (CRC) calculation. The  $\alpha$ -particle transfer between the two  $^{12}\text{C}$  cores has been explicitly included and calculated using the standard procedure for such a process with the code FRESKO by Thompson [14].

In this short note we present only the results of the first order calculation with the inclusion of the  $\alpha$ -exchange term between the ground states. The full CRC calculation, which will include the indirect routes for  $\alpha$ -transfer via the  $2^+$  state in  $^{12}\text{C}$  (see Refs. [15, 16]), and applied to more data from the literature will be published later. First calculations and previous experience with the strong coupling to the inelastic states [15] have shown that in this case a strong renormalization of the real potential will be needed. The "bare" potential usually has to be chosen to be deeper, because the effect of the inelastic coupling is a repulsive contribution, which makes the local effective op-

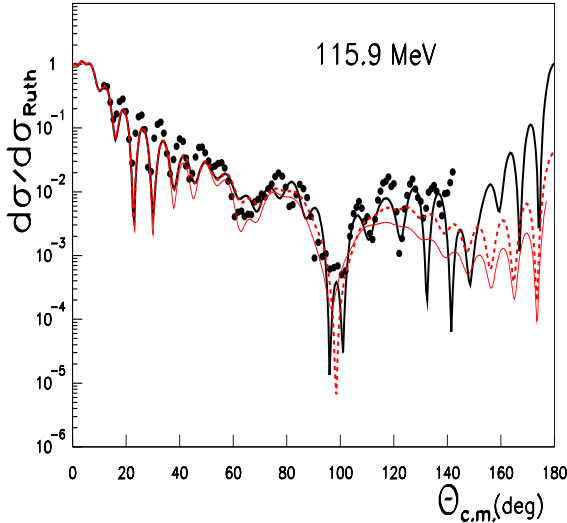


**Fig. 1.** Measured elastic scattering angular distribution displayed as ratio to the Rutherford scattering for  $^{16}\text{O}+^{12}\text{C}$  at an  $^{16}\text{O}$  incident energy of 115.9 MeV. The dashed curve represents the optical-potential calculation with parameters listed in Table 1, while the thick solid curve represents the first order CRC calculation with the inclusion of the elastic  $\alpha$ -particle exchange term. The thin solid curve represents the optical-potential fit with the parameters from Table II in Ref.[12].

tical potential less attractive. This bare potential for the CRC-calculation has to be searched in the fitting procedure, and the final calculation will take considerable time if several energies are analyzed.

The angular distribution measured at 115.9 MeV is a typical example for the features of the elastic cross section in this intermediate energy range between 5 and 10 MeV per nucleon. The resonant phenomena show up at lower energies while at higher energies the prominent appearance of the primary nuclear rainbow (Airy - maximum) has been observed. Here we observe higher order Airy structures, which are controlled by the strongly refractive real potential. The appearance of refractive effects removes the ambiguities in the determination of the optical potential. The strong real potential and the weakly absorptive imaginary part, which reflects the transparency, make the observation of higher order Airy minima possible. This is discussed in Refs. [5,12]. Figure 1 shows the elastic scattering angular distribution at 115.9 MeV together with the optical model fit using only the volume imaginary term for the absorptive potential (dashed curve), and the same potential together with the  $\alpha$ -transfer exchange within the CRC calculation (thick solid curve). The dashed curve describes well the broad structure of refractive origin, particularly the minima at  $65^\circ$  and  $100^\circ$ , which are identified as the third ( $A_3$ ) and second ( $A_2$ ) Airy minima respectively, forward of the primary rainbow [12]. These minima will move forward in angle as the energy increases (at 124 MeV the  $A_3$  and  $A_2$  minima are

**Table 1.** Phenomenological optical model potentials, the real part ( $V$  and the parameters with subscript  $V$ ) is a WS2 term, the imaginary part ( $W$  and the subscripts  $W$ ) refer to a WS1 term (pure volume).  $R$  and  $a$  stand for the radius and diffuseness. See Ref. [12] for more details.

$^{16}\text{O}+^{12}\text{C}$ $R_V=4$ fm, $a_V=1.4$ fm				
$E_{\text{lab}}$	$V$	$W$	$R_W$	$a_W$
[MeV]	[MeV]	[MeV]	[fm]	[fm]
124	285	11.8	5.72	0.636
115.9	290	11.5	5.88	0.522
100	288	9.0	5.92	0.553

located at  $60^\circ$  and  $90^\circ$ , while at 100 MeV they are at  $80^\circ$  and  $120^\circ$ ). The rise in the backward cross section and the oscillations superimposed on the broad structure are well reproduced when the transfer of an  $\alpha$ -cluster is included in the calculation (thick solid curve). There are some details in the observed oscillatory structure which are not reproduced, we believe that this part may be strongly influenced by the indirect route as mentioned before. The elastic  $\alpha$ -transfer also reduces the deepness of the  $A_2$  minimum predicted by phenomenological potential calculation alone.

The first order calculation is performed by including only the exchange between the ground state of  $^{12}\text{C}$ . The strength of the  $\alpha$ -exchange within this calculation must be treated as an effective value. Actually the pick-up process of an  $\alpha$ -particle from  $^{16}\text{O}$  gives the first excited state ( $2^+$ ) of  $^{12}\text{C}$  with a strength, which is four times stronger [17] than the ground state, a fact which emphasizes the need to include all coupling routes to the  $2^+$  state. The bound-state potential for the  $\alpha+^{12}\text{C}$  is of the Woods-Saxon type with the parameters:  $V=140$  MeV,  $r_0=1.1$  fm and  $a_0=0.5$  fm. The spectroscopic amplitudes for the overlaps between the ground states were used as 'fitting' parameters, because of the simplified coupling scheme. The resulting values for the spectroscopic amplitudes are:  $\langle ^{16}\text{O} | ^{12}\text{C} \rangle = 1.1$  (for 124 and 100 MeV) and 1.4 (for 115.9 MeV), the change of this factor with energy illustrates that the spectroscopic strength has to be considered as an effective measure for all exchange terms. The scattering potential for the elastic channel is the phenomenological optical potential obtained in Ref. [12] (the thin solid curves in figures 1 and 2). The exact parameters used are listed in Table 1. All parameters, except the depth of the imaginary part, are as reported in Ref. [12] (with only small changes) while the introduction of the exchange interaction tends to reduce the imaginary potential (the dashed curve in figure 1 shows the result). Indeed, the depths of the imaginary potentials needed are about 15 % smaller in this calculation when the  $\alpha$ -exchange term is included.

Figure 2 shows more elastic scattering data together with the first order CRC calculations for the  $^{16}\text{O}+^{12}\text{C}$  elastic angular distributions [7,12,13] at energies of  $E_{\text{LAB}}=124$ , 115.9 and 100 MeV, where the broad structures of refractive origin and the superimposed oscillations are pronounced. The measurements are well described by the calculation. The introduction of the exchange interaction

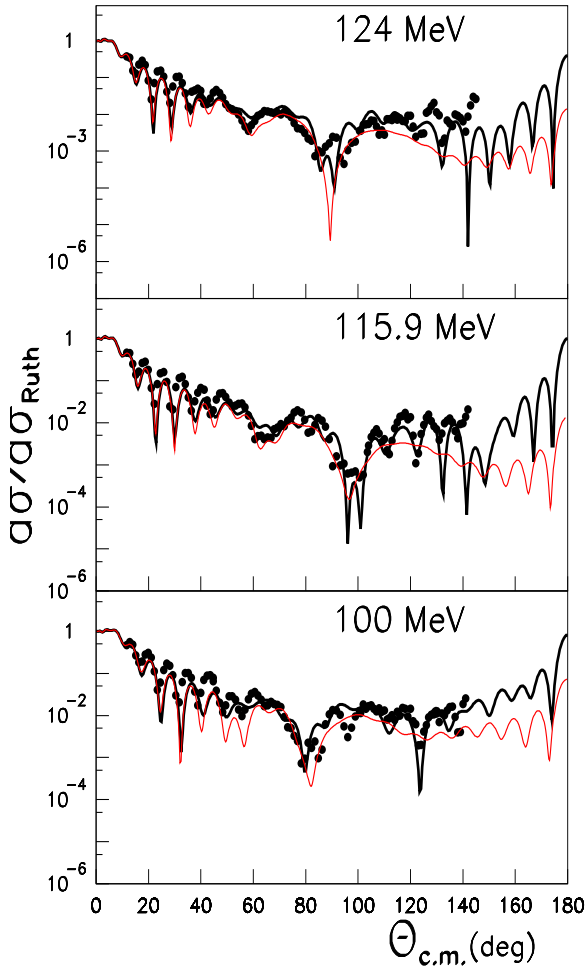


**Fig. 2.** Elastic scattering data shown as the ratio to the Rutherford cross sections and the results of fitting procedure with the optical model (thin curves) and the calculation with inclusion of the exchange interaction (thick curves) of  $^{16}\text{O}+^{12}\text{C}$  at energies  $E_{\text{LAB}} = 124, 115.9,$  and  $100$  MeV.

provides the increase as well as the oscillatory behavior at large angles. Such oscillatory structures are due to the interference of the direct elastic with the  $\alpha$ -exchange amplitudes. This additional analysis, where the elastic transfer is explicitly included, provides an understanding of the origin of the finer oscillations superimposed on the pronounced Airy structure at large angles in this intermediate energy range. It is expected that refined fits to the structure in the interference region may be achieved in a full CRC-calculation, where inelastic excitation of the  $^{12}\text{C}$  ( $2^+$  at  $4.43$  MeV) and the transfer via the  $2^+$  state will be incorporated. Such calculations have been done for other systems [15], and the analysis of the present data is in preparation.

#### ACKNOWLEDGMENTS

S.S. would like to express her gratitude to the Hahn-Meitner Institut, Berlin for the warm hospitality, as well as for the financial support.

#### References

1. F. Haas, and Y. Abe, *Phys. Rev. Lett.* **46**, 1667 (1981).
2. R.R. Betts, in *Proceedings of the 7th International Conference on Clustering Aspects of Nuclear Structure and Dynamics*, Rab, Croatia, 1999, edited by M. Korolija, Z. Basrak, and R. Čaplar (World Scientific, Singapore, 2000), p. 109 and references therein.
3. M.E. Brandan, and G.R. Satchler, *Phys. Rep.* **285**, 143 (1997) and references therein.
4. D.T. Khoa, W. von Oertzen, H.G. Bohlen, *Phys. Rev. C* **49**, 1652 (1994).
5. D.T. Khoa, W. von Oertzen, H.G. Bohlen and F. Nuoffer, *Nucl. Phys. A* **672**, 387 (2000).
6. M.P. Nicoli, F. Haas, R.M. Freeman, N. Aissaoui, C. Beck, A. Elanique, R. Nouicer, A. Morsad, S. Szilner, Z. Basrak, M.E. Brandan, and G.R. Satchler, *Phys. Rev. C* **60**, 064608 (1999).
7. M.P. Nicoli, F. Haas, R.M. Freeman, S. Szilner, Z. Basrak, A. Morsad, G.R. Satchler, and M.E. Brandan, *Phys. Rev. C* **61**, 034609 (2000).
8. A.A. Ogloblin, Yu. A. Glukhov, W.H. Trzaska, A.S. Dem'yanova, S.A. Goncharov, R. Julin, S.V. Klebnikov, M. Mutterstocker, M.V. Rozhkov, V.P. Rudakov, G.P. Tiorin, Dao T. Khoa, and G.R. Satchler, *Phys. Rev. C* **62**, 044601 (2000).
9. W. von Oertzen, *Nucl. Phys. A* **148**, 529 (1970).
10. W. von Oertzen and H.G. Bohlen, *Phys. Rep.* **19C**, 1 (1975) and references therein.
11. C. Gao, and Y. Kondō, *Phys. Lett. B* **408**, 7 (1997).
12. S. Szilner, M.P. Nicoli, Z. Basrak, R.M. Freeman, F. Haas, A. Morsad, M. E. Brandan, and G. R. Satchler, *Phys. Rev. C* **64**, 064614 (2001).
13. S. Szilner, Ph.D. thesis, Université Louis Pasteur, Strasbourg and University of Zagreb, 2001, Report No. IRoS 01-03.
14. I.J. Thompson, *Comp. Phys. Rep* **7**, 167 (1988).
15. I.V. Krouglov and W. von Oertzen, *Eur.Phys. J.A* **8**, 501 (2000).
16. R.J. Ascutto and E.A. Seglie, in: *Treatise on Heavy-Ion Science*, vol. 1, eds. D.A. Bromley (Plenum Press, New York, 1984).
17. F. Ajzenberg-Selove and J.H. Kelly, *Nucl. Phys. A* **506**, 1 (2000).